Electronic Supplementary Material (ESI) for Inorganic Chemistry Frontiers.

Supporting Information

CoS_2@montmorillonite as an efficient separator coating for high-performance lithium-sulfur batteries

Lian Wu,[a] Yifang Zhao,[a] Yongqiang Dai,[a] Shuxi Gao,[a] Bing Liao*[b] and Hao Pang*[a]

[a] Guangdong Provincial Key Laboratory of Industrial Surfactant, Institute of Chemical Engineering, Guangdong Academy of Sciences, Guangzhou 510665, Guangdong, P. R. China. *E-mail: panghao@gdcri.com*

[b] Guangdong Academy of Sciences, Guangzhou 510070, Guangdong, P. R. China. *E-mail: liaobing@gic.ac.cn*

Contents

Additional experiment section

Determination of electrolyte uptake

The modified and unmodified separators were soaked in the electrolyte (1.0 M lithium bis(trifluoro-methanesulfonyl)imide (LiTFSI) and 2 wt % $LiNO_3$ in dimethoxyethane and dioxolane (DME/DOL) mixed solvent (1:1, v/v)) for 2 min. Excess amounts of the electrolyte droplets remaining on the separator surface were removed by scraping with a small brush. The electrolyte uptake (wt%) was calculated by the following equation (Eq. S1).[1]

$$\textit{Electrolyte uptake}\ (\%) = (W - W_0)/W_0 \times 100\% \qquad \text{(Eq. S1)}$$

where W_0 and W is the weight of the separator before and after soaked in electrolyte, respectively.

Lithium-ion diffusion behavior characterization

(1) Lithium ions transference number

The modified/unmodified separators were separately sandwiched between two lithium metal electrodes in CR2025 coin cells with 30 μL Li-S battery electrolyte adding in each side of the separators. The lithium ions transference numbers of the separators were determined via chronoamperometry at a constant step potential of 10 mV and calculated by the following equation (Eq. S2).[2]

$$t_{Li^+} = I_s/I_o \qquad \text{(Eq. S2)}$$

where t_{Li^+} is the lithium ions transference number; I_o and I_s is the initial and steady current value, respectively.

(2) Ionic conductivity

The modified/unmodified separators were separately sandwiched between two stainless-steel electrodes in CR2025 coin cells with sufficient Li-S battery electrolyte. The ionic conductivities of the separators were determined by electrochemical impedance spectroscopy (EIS) from 100 kHz to 10 mHz with a potentiostatic amplitude of 5 mV and calculated by the following equation (Eq. S3).[2]

$$\sigma = \delta / (R_b \cdot A) \qquad \text{(Eq. S3)}$$

where σ is the ionic conductivity; δ is the thickness of the separator; R_b is the bulk resistance; A is the area of the stainless-steel electrode.

(3) Lithium-ion diffusion coefficient

CR2025 coin cells with the S/C cathodes, modified/unmodified separators, Li-S battery electrolyte, and lithium metal anodes were assembled. The lithium-ion diffusion coefficients of the separators were measured by performing a series of cyclic voltammograms (CV) tests at different scan rates and calculated according to the Randles-Sevick equation (Eq. S4).[3]

$$I_P = 2.69\times10^5 \cdot n^{3/2} \cdot A \cdot D_{Li}^{1/2} \cdot C_{Li} \cdot V^{1/2} \qquad \text{(Eq. S4)}$$

where I_P is the cathodic/anodic peak current; n is the charge transfer number (n = 2 for Li-S battery); A is the active electrode area (≈1.13 cm^2), D_{Li} is the Li ion diffusion coefficient; C_{Li} is the Li ion concentration in the electrolyte (10^{-3} mol·cm^{-3}); V is the scan rate.

Catalytic effect evaluation

The catalytic effect of the CoS_2@montmorillonite composite on polysulfide conversion was tested by assembling CR2025-type symmetric cells with two identical electrodes, pristine PP separator and 40 μL Li_2S_6 electrolyte (0.5 M). The electrodes were made by coating the prepared CoS_2@montmorillonite slurry on the aluminum foil. The areal mass loading was ~0.5 mg cm^{-2}. The Li_2S_6 electrolyte (0.5 M) was prepared by dissolving 230 mg Li_2S and 800 mg S in the 10 mL LiTFSI electrolyte. The CV curves were recorded in a voltage window of -1.5 to 1.5 V at a scan rate of 5 mV s^{-1}. The EIS measurements were carried out in the frequency range of 10^{-1} to 10^5 Hz using with a perturbation amplitude of 5 mV.

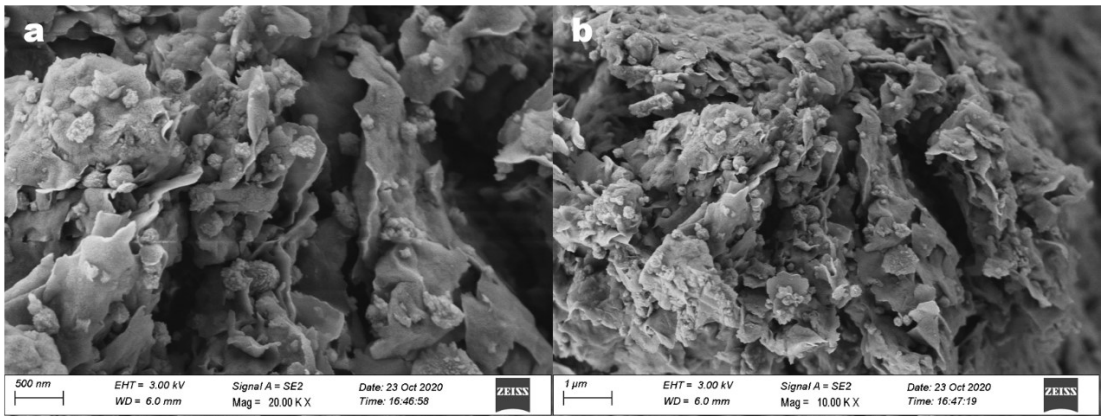

Fig. S1 SEM images of CoS_2@montmorillonite.

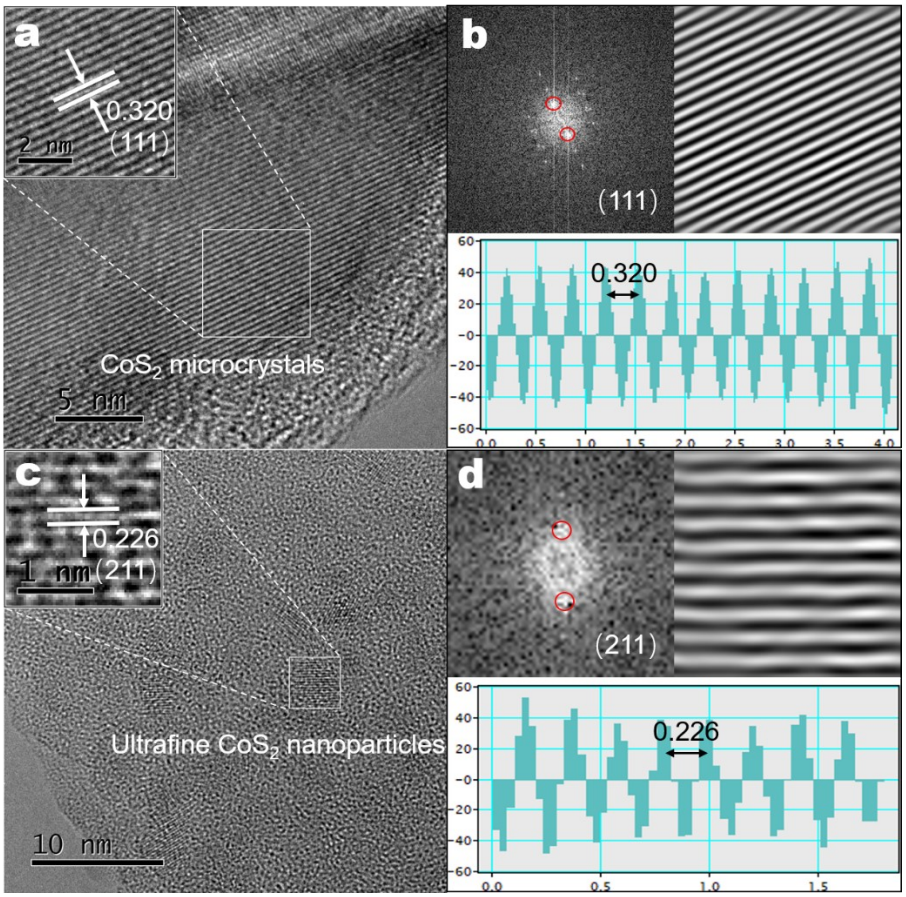

Fig. S2 HRTEM images of (a) the CoS_2 microcrystals on the surface of montmorillonite, (c) the CoS_2 nanoparticles in the interlayers of montmorillonite. (b,d) FFT images and intensity profile along the lines taken from (111) and (211) planes of CoS_2.

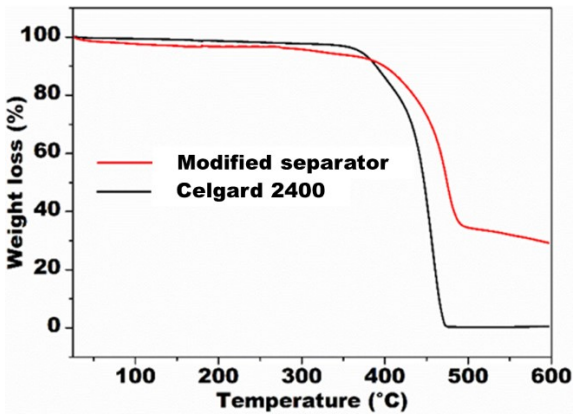

Fig. S3 TGA curves of Celgard 2400 and CoS_2@montmorillonite modified separators.

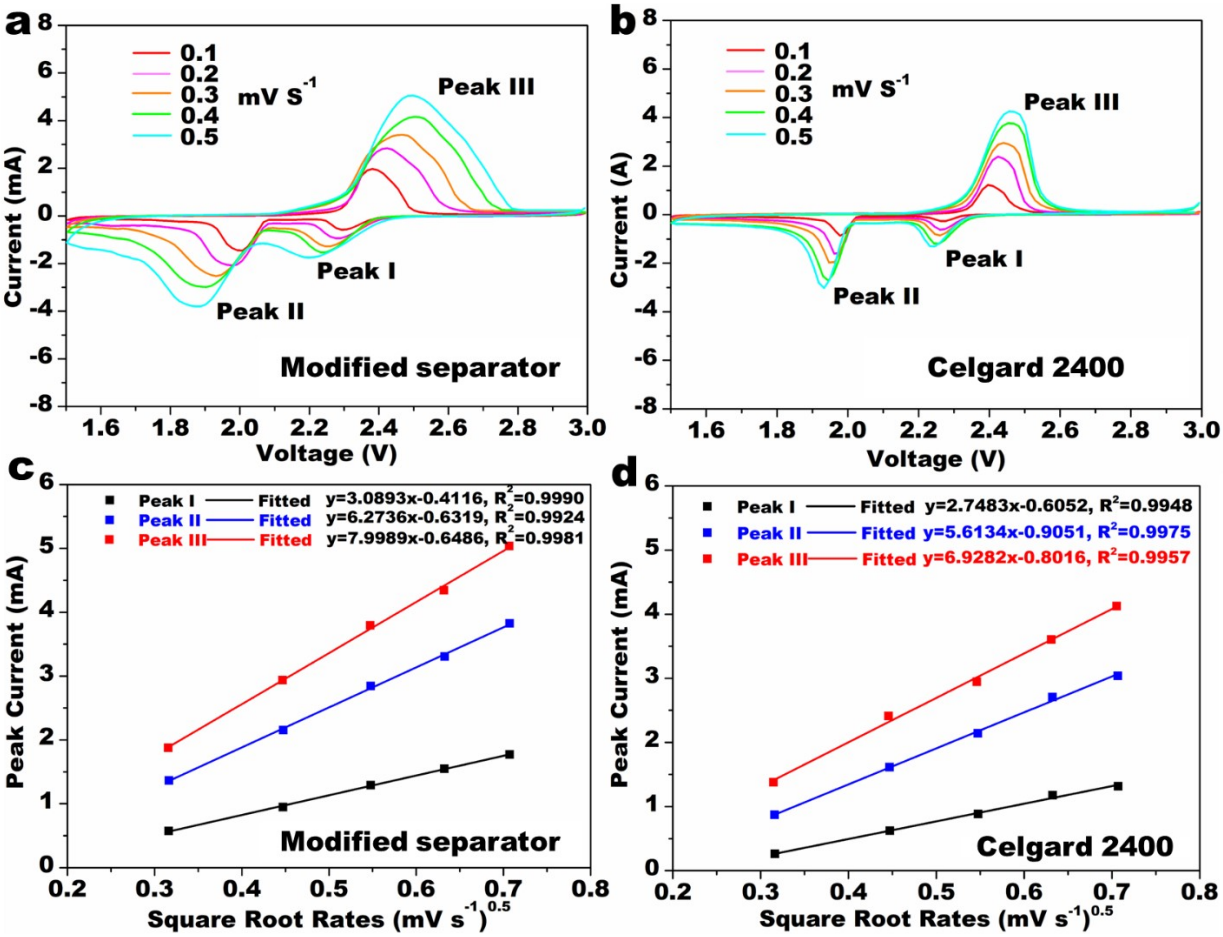

Fig. S4 CV curves of the cells with (a) CoS_2@montmorillonite modified separator and (b) Celgard 2400 separator at various scan rates and (c-d) their corresponding linear fits of peak currents with the square root of the scan rates.

Table S1 Values of R_s, R_{ct}, and W_C for various Li-S cells.

Separator used in the Li-S cell	R_s (Ω)	R_{ct} (Ω)	W_C (Ω)
CoS_2@montmorillonite modified separator	3.4	87	32
Celgard 2400	2.4	106	58

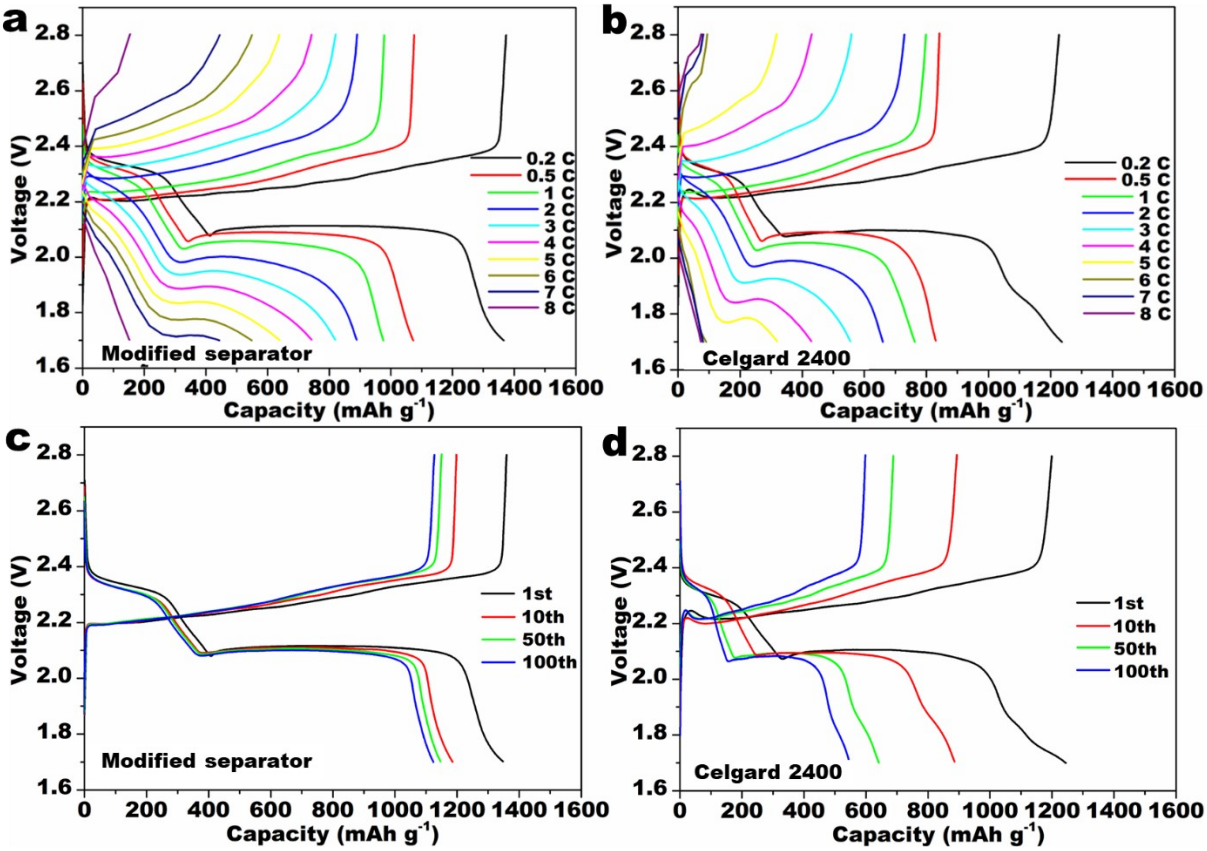

Fig. S5 Galvanostatic charge/discharge profiles of the cells with CoS_2@montmorillonite modified separator and Celgard 2400 separator at (a, b) various current rates and (c, d) at various cycles at 0.2 C.

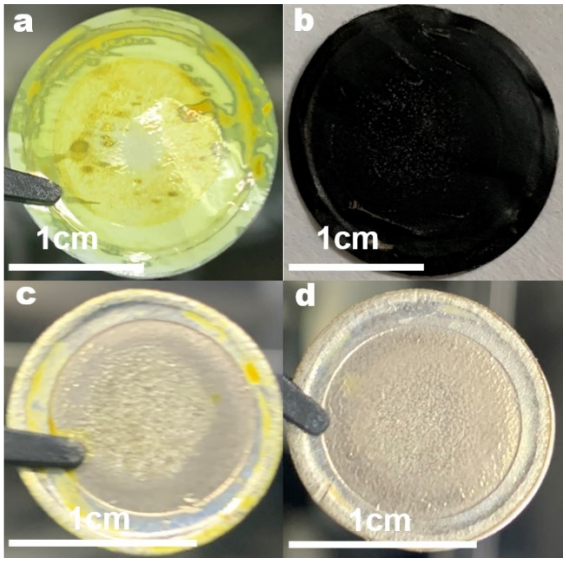

Fig. S6 Optical images of the (a) Celgard 2400, (b) modified separator, (c) lithium anode in the cells with Celgard 2400 separator, and (d) lithium anode in the cells with the modified separator after 40 cycles at 0.2 C.

Table S2 Comparison of electrochemical performance between this work and previous works.

Coating layer	Cathode	Sulfur loading (mg cm^{-2})	Rate performance (C, mAh g^{-1})	Cycling performance			References
				Current rate (C)	Cycles	Reversible capacity (mAh g^{-1})	
$(PEI/MMT/PAA)_5$	KB/S	1.5	1 C, 335	0.5	200	560	[1]
PPY/Li-MMT	AB/S	1.0	3 C, 540	0.6	600	606	[4]
MMT@C	AB/S	2.6	0.7 C, 684	0.23	300	818	[5]
		4.5	\	0.25	90	700	
MMT	MWCNTs/S	0.7	\	0.06	200	924	[6]
Li-MMT	AB/S	1.5	\	0.2	190	776	[7]
PVA/LRD	CB/S	1.0	3 C, 578	2	500	600	[8]
		5.4	\	1	400	712	
Illite-smectite/C	CNT/S	1.3-1.5	2 C, 702	1	500	626	[9]
		8.9	\	0.02	100	419	
NSPCF@CoS_2	Super P/S	1.2	4 C, 565.4	0.5	100	665.1	[10]
		2.04	2 C, 489.4	\	\	\	
NSPCFS@CoS_2	Super P/S	1.2	4 C, 271.7	0.5	100	631.6	[11]
CoSx QD-NSC	Super P/S	1.6	3 C, 640	1	1000	462	[12]
AB-CoS_2	AB/S	1.5	4 C, 475	2	450	380	[13]
CoS_2/HPGC	HPGC/Super P/S	3.0	2 C, 650	1	500	519	[14]
MXene-CoS_2	CNT/S	1.2	4 C, 775	1	700	651	[15]
		2.5	\	1	200	753	
P-CoS_2	CNT/S	1.1-1.4	5 C, 802.6	2	580	635.5	[16]
		4.8	\	0.2	100	937.5	
CoS@g-C_3N_4/KB	KB/S	1.5	2 C, 690	1	500	572	[17]
		4.0	\	0.1	250	600	
Co_4S_3/C@CC	CNT/S	1.1-1.5	10 C, 368.7	2	1400	360.6	[18]
		4.6	\	0.2	100	915.2	
CoS_2@ montmorillonite	**KB/S**	**1.0**	**7 C, 446**	**0.2**	**200**	**1090**	**This work**
				2	**1000**	**676**	
		4.0	**3 C, 595**	**0.2**	**100**	**853**	

References

[1] A. Mentbayeva, S. Sukhishvili, M. Naizakarayev, N. Batyrgali, Z. Seitzhan and Z. Bakenov, Ultrathin clay-containing layer-by-layer separator coating enhances performance of lithium-sulfur batteries, *Electrochim. Acta*, 2021, **366**, 137454.

[2] S. Ruan, Z. Huang, W. Cai, C. Ma, X. Liu, J. Wang, W. Qiao and L. Ling, Enabling rapid polysulfide conversion kinetics by using functionalized carbon nanosheets as metal-free electrocatalysts in durable lithium-sulfur batteries, *Chem. Eng. J.*, 2020, **385**, 123840.

[3] X. Tao, J. Wang, C. Liu, H. Wang, H. Yao, G. Zheng, Z. W. Seh, Q. Cai, W. Li, G. Zhou, C. Zu and Y. Cui, Balancing surface adsorption and diffusion of lithium-polysulfides on nonconductive oxides for lithium-sulfur battery design, *Nat. Commun.*, 2016, **7**, 11203.

[4] M. Yang, J. Nan, W. Chen, A. Hu, H. Sun, Y. Chen and C. Wu, Interfacial engineering of polypropylene separator with outstanding high-temperature stability for highly safe and stable lithium-sulfur batteries, *Electrochem. Commun.*, 2021, **125**, 106971.

[5] M. Yang, Z. Li, W. Chen, Y. Hu and Y. Yan, Carbon-intercalated montmorillonite as efficient polysulfide mediator for enhancing the performance of lithium-sulfur batteries, *Energy Fuels*, 2020, **34**, 8947-8955.

[6] W. Ahn, S. N. Lim, D. U. Lee, K. B. Kim, Z. W. Chen and S. H. Yeon, Interaction mechanism between a functionalized protective layer and dissolved polysulfide for extended cycle life of lithium sulfur batteries, *J. Mater. Chem. A*, 2015, **3**, 9461-9467.

[7] M. Yang, N. Jue, Y. Chen and Y. Wang, Improving cyclability of lithium metal anode via constructing atomic interlamellar ion channel for lithium sulfur battery *Nanoscale Res. Lett.*, 2021, **16**, 52.

[8] Y. Yang and J. Zhang, Layered nanocomposite separators enabling dendrite-free lithium metal anodes at ultrahigh current density and cycling capacity, *Energy Storage Mater.*, 2021, **37**, 135-142.

[9] W. Wang, Y. Yang, H. Luo, S. Li and J. Zhang, A separator based on natural illite/smectite clay for highly stable lithium-sulfur batteries, *J. Colloid Interf. Sci.*, 2020, **576**, 404-411.

[10] N. Wu, J. Wang, C. Liao, L. Han, L. Song, Y. Hu, X. Mu and Y. Kan, A flame retardant separator modified by MOFs-derived hybrid for safe and efficient Li-S batteries, *J. Energy Chem.*, 2022, **64**, 372-384.

[11] J. Wang, W. Cai, X. Mu, L. Han, N. Wu, C. Liao, Y. Kan and Y. Hu, Construction of multifunctional and flame retardant separator towards stable lithium-sulfur batteries with high safety, *Chem. Eng. J.*, 2021, **416**, 129087.

[12] H. Lu, Q. Guo, Q. Fan, L. Xue, X. Lu, F. Zan and H. Xia, Cobalt sulfide quantum dot embedded in nitrogen/sulfur-doped carbon nanosheets as a polysulfide barrier in Li-S batteries, *J. Alloy. Compd.*, 2021, **870**, 159341.

[13] P. Zeng, L. Huang, X. Zhang, Y. Han and Y. Chen, Inhibiting polysulfides diffusion of lithium-sulfur batteries using an acetylene black-CoS_2 modified separator: Mechanism research and performance improvement, *Appl. Surf. Sci.*, 2018, **427**, 242-252.

[14] Q. Hu, J. Lu, C. Yang, C. Zhang, J. Hu, S. Chang, H. Dong, C. Wu, Y. Hong and L. Zhang, Promoting reversible redox kinetics by separator architectures based on CoS2/HPGC interlayer as efficient polysulfide-trapping shield for Li-S batteries, *Small*, 2020, **16**, 2002046.

[15] C. Yang, Y. Li, W. Peng, F. Zhang and X. Fan, In situ N-doped CoS_2 anchored on MXene toward an efficient bifunctional catalyst for enhanced lithium-sulfur batteries, *Chem. Eng. J.*, 2022, **427**, 131792.

[16] J. Liu, Z. Qiao, Q. Xie, D. L. Peng, and R. J. Xie, Phosphorus-doped metal-organic framework-derived CoS_2 nanoboxes with improved adsorption-catalysis effect for Li-S batteries, *ACS Appl. Mater. Interfaces*, 2021, **13**, 15226-15236.

[17] X. Liu, S. Wang, H. Duan, Y. Deng and G. Chen, A thin and multifunctional CoS@g-C_3N_4/Ketjen black interlayer deposited on polypropylene separator for boosting the performance of lithium-sulfur batteries, *J. Colloid Interf. Sci.*, 2022, **608**, 470-481.

[18] J. Liu, Y. Song, C. Lin, Q. Xie, D. L. Peng and R. J. Xie, Regulating Li^+ migration and Li_2S deposition by metal-organic framework-derived Co_4S_3-embedded carbon nanoarrays for durable lithium-sulfur batteries, *Sci. China Mater.*, 2022, **65**, 947-957.